# STATE SPACE MODELLING OF MULTIVARIATE DYNAMIC PROCESS SYSTEMS BY USE OF INDEPENDENT COMPONENT ANALYSIS

*J. P. Barnard and C. Aldrich*

Department of Chemical Engineering, University of Stellenbosch,

Private Bag X1, Matieland, Stellenbosch, South Africa, 7602.

Email: *jsteyl@ing.sun.ac.za* (secretary)

## Abstract

A novel method is defined to reconstruct the dynamic attractor by multidimensional embedding of observations of a dynamic, non-linear process. Takens' embedding theory is combined with independent component analysis to transform the embedding to a vector space of statistically independent vectors (state variables). The method of embedding was successfully tested, using various embedding strategies on data generated by a non-linear process in a chemical reactor as well atmospheric $NO_2$.

## Background

Embedding of observations in phase space is central to the analysis of non-linear dynamic process systems and the treatment of one-dimensional systems in this way is well-established in non-linear system identification [1]. However, identification of dynamic systems based on multi-dimensional observations has not been sufficiently formalised in terms of embedding theory, despite the practical importance of these types of systems. One cannot always predict the time evolution of a system state from a single observed variable [2]. For example, the Lorenz system [3] has three state variables, $x$ $y$ $z$, but $\dot{x} = f(x, y)$, while $\dot{z} = f(x, y, z)$, thus one cannot properly predict $z$ only from $x$ or even $(x,y)$-observations.

Cao et al. [2] proposed embedding all components of the multi-dimensional observations using an optimal Takens embedding for each component, by minimising the average prediction error of a nearest neighbour, locally constant predictor. Unfortunately Cao et al. [2] did not indicate how to optimise the embedding lag, which is crucial in the reconstruction of a representative attractor on realistic systems, especially if noise is present in the observations. Individual embedding of each observation could lead to significant statistical dependence between some of the embedded (lag) variables, resulting in an attractor that is not optimally reconstructed from the observations.

In this paper we therefore propose a novel method to embed multidimensional observations in chemical process systems that avoids both linear approximations in finding embedding dimensions and potentially sub-optimal embedding lags. With this approach, each component is treated as a one-dimensional time-series and embedded individually to generate a subspace. These subspaces are consequently combined to form a first approximation of the attractor in $\Re^{\Lambda} = [\Re^{m1}, \Re^{m2}, ..., \Re^{mM}]$. Finally, the lag variables are decorrelated to optimise the structure of the attractor. This result in a properly reconstructed dynamic attractor based on the observation space with optimally decorrelated state variables.

## Methodology

Let $\mathbf{Y} = [\mathbf{Y_1}, \mathbf{Y_2}, \mathbf{Y}_3, \cdots, \mathbf{Y}_N]^{\mathrm{T}}$ be the array of $p$-dimensional observations, where each $\mathbf{Y}_i = [y_{i1}, y_{i2}, y_{i3}, \ldots y_{ip}]$ for $i = 1, 2, 3, \ldots, N$. Multidimensional embedding of $\mathbf{Y}$, using

Takens' embedding [4], results in the embedding matrix **X,** where each element,

$$\mathbf{X}_{ij} = \left[ y_{i+k_j(m_j-1),j} \quad y_{i+k_j(m_j-2)_j,j} \quad ,\cdots, \quad y_{i,j} \right]$$
$$i = b_j \ldots N, j = 1 \ldots p$$
$$b_j = \max\left[k_j(m_j-1)\right] - k_j(m_j-1) + 1 \qquad (\mathbf{1})$$

with $k_j$, the embedding lag and $m_j$, the embedding dimension for each observation $\mathbf{Y}_j$. In this investigation, the embedding lag was determined by the average mutual information statistic [5] and the embedding dimension by the false nearest neighbours algorithm [6]. Possible statistical dependencies among lag variables are removed by optimal projection of **X** of the observations, as follows:

$$\mathbf{S} = \mathbf{WX} \qquad (\mathbf{2})$$

where **S** is the optimal projection of the original embedding and **W** the separating matrix. The dimension of **S** may be lower than that of **X.** Thus one may achieve optimal projection, reduction of dimensionality, as well as independence of the embedding variables.

Applying Hyvärinen's method [7] to find **W,** one has to maximise the negentropy $J_G$ of **X,** which is equivalent to minimising the mutual information among components of **X,** under the constraint of decorrelation of the components, that is:

$$\text{maximize} \sum_{i=1}^{M} J_G(\mathbf{w}_i) \text{ wrt. } \mathbf{w}_i, \qquad (\mathbf{3})$$

under the constraint,

$$E\{\mathbf{w}^{\mathrm{T}}{}_k \mathbf{w}^{\mathrm{T}}{}_j\} = \delta_{jk} \qquad (\mathbf{4})$$

where,

$$J_G(\mathbf{w}) = [E\{G(\mathbf{w}^{\mathrm{T}}\mathbf{x})\} - E\{G(\nu)\}]^2 \qquad (\mathbf{5})$$

with $G(\cdot)$ some sufficiently smooth, even, so-called contrast function that estimates the probability density function of an independent component, *c* some insignificant constant, and *v* a standardised Gaussian variable. Each vector $\mathbf{w}_i$ , is a row of matrix **W.** The matrix **S** represents the attractor of the dynamic system.

## Case study 1: Modelling of non-isothermal CSTR reaction

We first demonstrate the embedding method in a case study of a non-linear exothermal reaction process (A→B), that runs in a non-isothermal Continuously-Stirred Tank Reactor (CSTR) [8]. The process can be described in terms of the following set of differential equations:

$$\frac{\mathrm{d}C_A}{\mathrm{d}t} = \frac{q}{V}\left(C_{Af} - C_A\right) - k_0 C_A \exp\left(-\frac{E}{RT}\right)$$
$$\frac{\mathrm{d}T}{\mathrm{d}t} = \frac{q}{V}\left(T_f - T\right) + \frac{(-\Delta H)k_0 C_A}{\rho C_p}\exp\left(\frac{E}{RT}\right)$$
$$+ \frac{\rho_c C_{pc}}{\rho C_p V} q_c \left[1 - \exp\left(-\frac{hA}{q_c \rho C_{pc}}\right)\right]\left(T_{cf} - T\right) \qquad (\mathbf{6})$$

where $C_A$ is effluent concentration; $T$, reaction temperature, $q_c$, coolant flow rate; $q$, feed flow rate; $C_{Af}$, feed concentration; $T_f$, feed temperature; $T_{cf}$, coolant inlet temperature. Table I defines the remaining model parameters, as well as the nominal operating conditions and initial conditions.

Using various embedding strategies, four different parameterisations of the process dynamics were performed and used to predict the effluent concentration one step ahead. These were: (1) the trivial embedding of effluent concentration and reaction temperature; (2) embedding of the effluent concentration only; (3) a multidimensional embedding of effluent concentration and reaction temperature, not optimised by independent component analysis; and (4) the same multidimensional embedding as in (3), but optimised by independent component analysis.

For the settings in Table I, the authors solved the set of equations (**6**), using a 5th order Runge Kutta numerical method over 1000 simulated

seconds. This gave 4705 points, which were re-sampled with constant sampling period of 0.1 s to give 10000 two-dimensional observations in effluent concentration and reaction temperature.

**Table I Parameters for nominal CSTR operating conditions [8].**

| | |
|---|---|
| q | 100 [L $min^{-1}$] |
| $C_{Af}$ | 1 [mol $L^{-1}$] |
| $T_f$ | 350 [K] |
| $T_{cf}$ | 350 [K] |
| V | 100 [L] |
| hA | $7\times10^5$ [cal $min^{-1}$ $K^{-1}$] |
| $k_0$ | $7.2\times10^{10}$ [$min^{-1}$] |
| E/R | $9.95\times10^3$ [K] |
| $-\Delta H$ | $2\times10^5$ [cal $mol^{-1}$] |
| $\rho$, $\rho_c$ | 1000 [g $L^{-1}$] |
| $C_p$, $C_{pc}$ | 1 [cal $g^{-1}$ $K^{-1}$] |
| $q_c$ | 103.41 [L $min^{-1}$] |
| T | 440.2 [K] |
| $C_A$ | $8.36\times10^{-2}$ [mol $L^{-1}$] |

According to the trivial embedding strategy of the first parameterisation, an embedding lag, $k = 1$, and dimension, $m = 1$, were used to embed $C_A$ and $T$. This means the observed process states, $C_A$ and $T$ , were used direct to predict $C_A$ one step ahead from the current observation. According to the embedding strategy of parameterisation (2), $C_A$ only was embedded. average mutual information calculations indicated an embedding lag, $k$ = 6, and false nearest neighbours calculations suggested an optimal embedding dimension, $m$ = 4. After some trial and error by trying several embeddings of different lags to predict $C_A$, it appeared that the optimal embedding lag was $k$ = 1. Consequently, this lag was used throughout the rest of the investigation.

For parameterisations (3) and (4), the first step of the proposed multidimensional embedding strategy was to embed the individual observation components, $C_A$ and $T$. average mutual information and false nearest neighbours calculations were performed for $C_A$ and T individually. An embedding lag, $k$ = 1 and embedding dimension, $m$ = 4 were used for the embedding of both $C_A$ and $T$. Combining the subspaces that resulted from individual embedding of $C_A$ and $T$, gave an $\Re^8$-embedding space. For parameterisation (3), the combined embedding space was used direct to predict $C_A$ one step ahead. On the other hand, for parameterisation (4), Hyvärinen's method [7] with a contrast function of the form $G(s) = (1/\alpha)\log\cosh(\alpha s)$ and $\alpha$ some constant, was used to obtain an optimal projection of the embedding space.

For all parameterisations, prediction of $C_A$ was done by using a multilayer perceptron neural network with a single hidden layer consisting of 15 hyperbolic tangent nodes and a single-node linear output layer. The size of the hidden layer was determined by iterative training and testing of networks using progressively larger numbers of nodes in the hidden layer. The parameters of the network were estimated with the Levenberg-Marquardt algorithm on the first 8000 observations, tested against observations 8001 to 9000 and finally validated once only against observations 9001 to 10000. The $R^2$-statistic, $R^2 = 1 - \sum \frac{y - \hat{y}}{(n\text{-}1)s^2(y)}$, was selected as fitness criterion, where $y$ is the observation and $\hat{y}$, the prediction of $y$; $n$, the number of observations; and $s^2$, the sample variance of the observations.

The $R^2$ results for the various parameterisations are shown in Table II, while figure 1 shows the results for parameterisation (4). It is clear from Table II that the multidimensional embedding strategy proposed in this paper is the best of the parameterisations investigated for this process system. Parameterisation (4) scored the highest $R^2$ = 0.975 of all. Parameterisation (3) fared

about the same as (2), while (1), using the trivial embedding, scored the worst. The improvement of parameterisation (4) over each of the other parameterisations was statistically significant in each case, based on a two-tailed hypothesis test on the Fisher transformation of $r = \sqrt{R^2}$ .

**Case study 2: Modelling of air pollution in Cape Town metropole**

We next selected air pollution in the Cape Town metropolitan area in South Africa as a basis for the second case study. A data set was kindly provided by the Cape Town Metropolitan Scientific Services. The data set contained 8664 records of synchronised, hourly mean concentrations of NO, $NO_2$, ambient temperature and solar radiation for the city centre of Cape Town, observed during 1996.

Classification of the $NO_2$ data, using a surrogate data method [9,10], showed the data to be nearly random. Noise filtering was not performed. However, outliers were removed by constructing a convex hull around the full variable space consisting of [$X_{NO2}$, $X_{NO}$, $X_{Es}$] and removing the hull. A total of 452 outliers were so removed.

$NO_2$ concentration ($X_{NO2}$) was chosen as the dependent variable with the aim to make acceptable one-step predictions in terms of NO concentration ($X_{NO}$) and solar radiation ($X_{Es}$). The first 6000 records were selected for fitting a non-linear model. A test set of records 6001 to 7000 was used for the optimisation of model order. Final models were validated on records 7001 to 8000.

Parameterisation of the system was investigated in terms of two alternative embedding strategies and associated model structures. The first strategy implied embedding all observation components using optimal individual embeddings summarised in Table III. The individual embeddings were combined as $\Lambda_1 \in \Re^{17}$ and separated as $S_1=W_1\Lambda_1$ by ICA with the power-3 contrast function. Consequently, the following model was constructed:

$$S_1(t) \rightarrow X_{NO2}(t+1) \qquad (7)$$

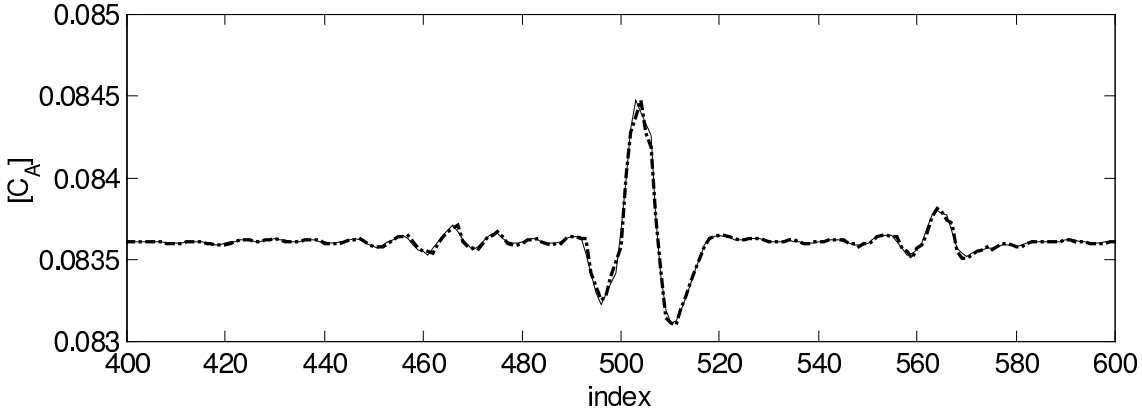


**Figure 1 Prediction of concentration, $C_A$, based on parameterisation (4), using a multilayer perceptron neural network. The dashed line is the prediction.**

**Table II** $R^2$ **statistic for prediction of** $C_A$ **, for various parameterisations of the process.**

| Parameterisation | State space dimension | Optimally projected | $R^2$ |
|---|---|---|---|
| Parameterisation (1) | 2 | no | **0.908** |
| Parameterisation (2) | 4 | no | **0.963** |
| Parameterisation (3) | 8 | no | **0.965** |
| Parameterisation (4) | 8 | yes | **0.975** |

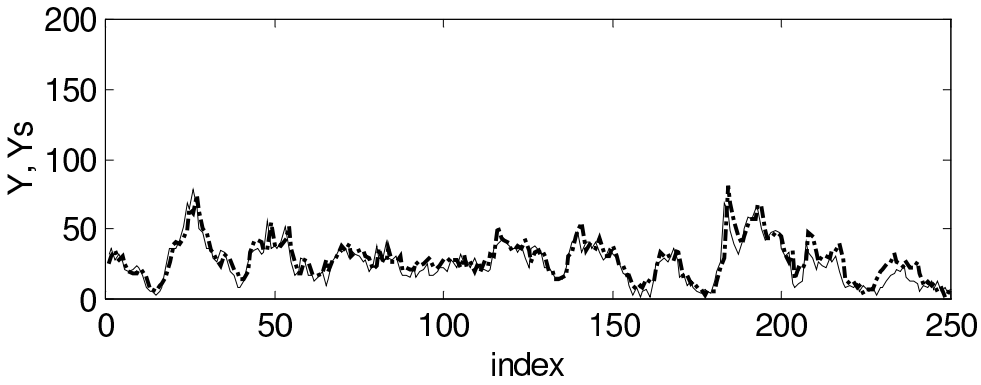


**Figure 2 Prediction of atmospheric $NO_2$ concentration (dashed line) in validation data set, using a multi-layer perceptron network with parameterisation strategy 1.**

In accordance with the second embedding strategy, no variables were embedded, resulting in the following model:

$$[X_{NO}\ X_{Es}] \rightarrow X_{NO2}(t+1) \qquad (8)$$

Multi-layer perceptron model structures with single hidden layers, consisting of bipolar sigmoidal nodes, were selected in all cases. In addition, a linear output layer was used in each case. The network parameters were estimated by using the Levenberg-Marquardt algorithm.

Model order was increased iteratively from 2 to 16 hidden nodes and the $R^2$-statistic calculated for the prediction of $X_{NO2}$ in the test set. The optimal model order was found to be 8 hidden nodes for both the embedding strategies.

Prediction of $X_{NO2}$ from the validation data set, using parameterisation strategy 1, resulted in an $R^2$ of 0.794, while strategy 2 only managed an $R^2$ of 0.737. As with the first case study, the improved performance of the first strategy was shown to be statistically significant.

## Conclusions

Based on the case studies discussed above, as well as other experiments not reported here, we can conclude that the proposed parameterisation technique of multivariate embedding, using independent component analysis, can make a significant contribution to the modelling of multivariate dynamic systems.

**Table III Embedding parameters for air pollution data: strategy 1**

| | $NO_2$ | NO | $E_s$ |
|---|---|---|---|
| **m** | 5 | 5 | 7 |
| **k** | 9 | 14 | 9 |


[1] M. Small, K. Judd, Comparison of new non-linear modelling techniques with applications to infant respiration, *Physica D*, **117**, 283, (1998).

[2] L. Cao, A. Mees, K. Judd, Dynamics from multivariate time series, *Physica D*, **121**, 75, (1998).

[3] E. N.Lorenz, Deterministic non-periodic flows, *J. Atmos. Sci*, **20,** 131, (1963).

[4] F. Takens, Detecting strange attractors in turbulence, *Lecture notes in Mathematics*, **898**, Springer (Berlin), 366, (1981).

[5] A. M. Frazer, H. L. Swinney, Independent coordinates for strange attractors, *Physical Review*, **33A**, 1134, (1986).

[6] M.B. Kennel, R. Brown, and H.D.I. Abarbanel, Determining minimum embedding dimension using a geometrical construction, *Physica Review A,* **45**, 3403, (1992).

[7] A. Hyvärinen, Independent component analysis by minimisation of mutual information, *IEEE Transactions on Neural Networks*, **10**, 626, (1999).

[8] E.P. Nahas, M.A. Henson, and D.E. Seborg, Nonlinear, internal model control strategy for neural network models, *Computers and Chemical Engineering*, **16**, 1039, (1992).

[9] K. Judd and A. Mees, On selecting models for non-linear time series, *Physica D*, **82**, 426-444, (1995).

[10] J. Theiler, E. Eubank, A. Longtin and B. Galdrikian, Testing for non-linearity in time series: The method of surrogate data, *Physica*, **58D**, 77-94, (1992).